Glutaminyl Cyclase Knock-out Mice Exhibit Slight Hypothyroidism but No Hypogonadism
IMPLICATIONS FOR ENZYME FUNCTION AND DRUG DEVELOPMENT*[S]

Stephan Schilling[‡1,2], **Stephanie Kohlmann**[§1], **Christoph Bäuscher**[§1], **Reinhard Sedlmeier**[§], **Birgit Koch**[‡], **Rico Eichentopf**[‡], **Andreas Becker**[§], **Holger Cynis**[‡], **Torsten Hoffmann**[‡], **Sabine Berg**[¶], **Ernst-Joachim Freyse**[¶], **Stephan von Hörsten**[‖], **Steffen Rossner**[**], **Sigrid Graubner**[§3], **and Hans-Ulrich Demuth**[‡§]

From ‡*Probiodrug AG, Weinbergweg 22, 06120 Halle/Saale,* §*Ingenium GmbH, Fraunhoferstrasse 13, 82152 Martinsried, the* ¶*Institute of Diabetes, "Gerhardt Katsch," 17495 Karlsburg, the* ‖*University of Erlangen-Nürnberg, Franz-Penzoldt-Center, Palmsanlage 5, 91054 Erlangen, and the* **Paul Flechsig Institute for Brain Research, University of Leipzig, Jahnallee 59, 04109 Leipzig, Germany*

Glutaminyl cyclases (QCs) catalyze the formation of pyroglutamate (pGlu) residues at the N terminus of peptides and proteins. Hypothalamic pGlu hormones, such as thyrotropin-releasing hormone and gonadotropin-releasing hormone are essential for regulation of metabolism and fertility in the hypothalamic pituitary thyroid and gonadal axes, respectively. Here, we analyzed the consequences of constitutive genetic QC ablation on endocrine functions and on the behavior of adult mice. Adult homozygous QC knock-out mice are fertile and behave indistinguishably from wild type mice in tests of motor function, cognition, general activity, and ingestion behavior. The QC knock-out results in a dramatic drop of enzyme activity in the brain, especially in hypothalamus and in plasma. Other peripheral organs like liver and spleen still contain QC activity, which is most likely caused by its homolog isoQC. The serum gonadotropin-releasing hormone, TSH, and testosterone concentrations were not changed by QC depletion. The serum thyroxine was decreased by 24% in homozygous QC knock-out animals, suggesting a mild hypothyroidism. QC knock-out mice were indistinguishable from wild type with regard to blood glucose and glucose tolerance, thus differing from reports of thyrotropin-releasing hormone knock-out mice significantly. The results suggest a significant formation of the hypothalamic pGlu hormones by alternative mechanisms, like spontaneous cyclization or conversion by isoQC. The different effects of QC depletion on the hypothalamic pituitary thyroid and gonadal axes might indicate slightly different modes of substrate conversion of both enzymes. The absence of significant abnormalities in QC knock-out mice suggests the presence of a therapeutic window for suppression of QC activity in current drug development.

Proteolytic cleavage, glycosylation, and C-terminal amidation represent important post-translational modifications of proteins in the secretory pathway. Among these, several proteins and peptide hormones carry an N-terminal 5-oxoprolyl (pyroglutamate (pGlu)[4]) residue. Examples of pGlu-containing peptides include the hormones thyrotropin-releasing hormone (TRH) and gastrin, the neuropeptide neurotensin, and the human chemokines MCP-1 to -4 (monocyte chemotactic proteins 1–4) (1, 2). It has been suggested that the pGlu residue protects the proteins from cleavage by aminopeptidases. For TRH or MCP-1 or -2, the biological function has been shown to depend strictly on 5-oxoproline at the N terminus. Loss or modification of this residue leads to a decrease in biological activity due to a decreased receptor interaction (3–5). For most of the proteins, however, the function of the N-terminal modification remains to be clarified. The potential role of the pGlu modification of amyloid peptides, which are deposited in neurodegenerative disorders like Alzheimer disease, familial British dementia, and familial Danish dementia, has been described recently (6–8). Apparently, the N-terminal pGlu modification increases the amyloidogenicity of those peptides by changing the secondary structure and, importantly, their hydrophobicity (6, 9, 10). It appears likely that the modified peptide species are involved in disease progression. Thus, preventing N-terminal modification might represent a strategy for the development of potential novel treatment paradigms (11, 12).

Although it is well known that N-terminal glutaminyl residues tend to form pGlu by spontaneous deamidation (13), the reaction is catalyzed by glutaminyl cyclases (QCs; EC 2.3.2.5) *in vivo* (14). Two functional genes, *QPCT* (QC) and *QPCTL* (isoQC), encoding glutaminyl cyclases have been described in mammals (15–17). Although QC represents a secreted protein,

which is apparently involved in hormone maturation in neuroendocrine tissue (14, 18), the function of the recently identified isoQC still remains unclear. The retention of the isoenzyme in the Golgi complex might suggest a role in the constitutive protein maturation similar to that of glycosyltransferases (15).

In order to gain further insight into the role of QC in hormone maturation and its potential physiological importance, we aimed here at the generation of mice that are deficient in a functional *QPCT* gene. Homozygous mice do not show a phenotype or apparent malfunction, which has implications for current strategies to develop QC inhibitors as treatments for neurodegenerative disorders.

EXPERIMENTAL PROCEDURES

Mouse Lines and Animal Husbandry

All mice were maintained in individually ventilated cages at a temperature (22 ± 2 °C)- and humidity ($55 \pm 10\%$)-controlled facility with a 12-h light/dark cycle and had access to standard laboratory chow and water *ad libitum*. The 129SvPas/C57/Bl6 hybrid founders were crossed two times against C57/Bl6, yielding the genetic background of 87.5% C57/Bl6 and 12.5% 129SvPas. All experiments were performed in accordance with the German animal protection law.

Generation of QC-targeted ES Cells

The knock-out mice were generated by homologous recombination of a targeting vector in embryonic stem cells (ES cells) at genOway (Lyon, France). The targeting vector contained the mouse chromosomal QC region ranging from intron 3 to exon 6. This region was modified by the insertion of two LoxP sites in introns 3 and 5, respectively. In addition, a neomycin resistance cassette flanked by two flippase recognition targets was inserted immediately upstream of the LoxP site in intron 5. The linearized targeting vector was transfected into 129SvPas-derived ES cells by electroporation, and stably transfected cells were isolated by G418 selection. Resistant clones were screened for homologous recombination of the targeting vector by PCR amplification of the 3′ and 5′ integration sites. A restriction enzyme digestion of the PCR fragment allowed a reliable identification of the homologous recombination event. The results of the PCR screening were further verified by Southern blot hybridization.

Generation of Constitutive QC Knock-out Mice

Targeted ES cells were injected into blastocysts, and chimeras were generated by embryo transfer. For removal of the neomycin selection cassette, the chimeras were mated to Flp-expressing animals followed by breeding of the progeny with Cre-expressing animals for deletion of QPCT exons 4 and 5. Animals that were heterozygous for the *QPCT* locus were identified. These founders of the new pbd-02 line carry a *QPCT* allele, where exons 4 and 5 are deleted. In addition, deletion of exons 4 and 5 causes a frameshift in the *QPCT* open reading frame, generating a stop codon in exon 6. Thus, the complete C-terminal part of the QC protein is lost in the knock-out line.

Genotyping Protocol

For genotyping of the pbd-02 animals, an allele-specific PCR using a set of three primers was developed, which enabled all possible genotypes to be distinguished by the different size of the PCR products. The primer set contained the upstream primer Pbd2-1 (5′-GTCCGGTAAGGTGAGGAGAA-3′), which binds to QPCT intron 3, and the downstream primers Pbd2-WT1 (5′-CCAGAGACATCCTGGTAAAACA-3′) and Pbd2–2 (5′-TGATGTGTGCGTTTCAGAGA-3′), which bind to exon 4 and intron 5, respectively. A standard PCR (58 °C annealing temperature, 45 s extension time, 30 cycles) on chromosomal pbd-02 DNA clearly distinguished the wild type allele (single larger band; 735 bp), knock-out allele (single smaller band; 525 bp), and heterozygous DNA (both bands; see Fig. 1*A*).

Behavioral Analyses

Primary Screen—The primary screen was used to prompt animals' general health, neurological reflexes, and sensory functions (muscle and lower motor neuron functions and spinocerebellar, sensory, neuropsychiatric, and autonomic functions) that could interfere with further behavioral assays. It was based on the guidelines of the SHIRPA protocol, which provides a behavioral and functional profile by observational assessment (19). The investigation started with observing social behavior in the home cage ("home cage observation") and subsequently undisturbed behavior of single animals in a clear Plexiglas arena for 90 s ("individual observation"). This monitoring of mouse behavior was followed by a battery of short tests for further characterization: acoustic startle reflex, hanging behavior, visual placing, falling behavior, righting reflex, postural reflex, negative geotaxis, hanging wire, ear twitch, whisker twitch, and eye blink. Finally, the animal was examined for dysmorphological and weight abnormalities.

Contextual Fear Conditioning—Using an automated fear conditioning system (TSE Systems, Bad Homburg, Germany), memory of an aversive experience (associated learning) was explored by investigating contextual and cued fear responses via infrared sensor-based activity measurement. On the first day (conditioning trial) animals were placed individually in constantly illuminated ($\sim$300 lux), transparent Plexiglas chambers with a metal grid floor, housed within sound-attenuated boxes. A loudspeaker provided a constant, white background noise (68 dB SPL). After a 210-s habituation to the chamber, mice received an auditory cue (10 kHz, 75 dB SPL) for 30 s and an electric foot shock (0.7 mA constant current) for the final 2 s of the tone. 30 s after the foot shock, animals were returned to their home cages. On day 2, 24 h after the conditioning trial, contextual memory was tested by placing the animals in the familiar chamber without tone and foot shock and measuring their behavior during a 210-s trial period (context phase). 1 h later, after alteration of the testing chamber by using black, opaque Plexiglas boxes (leading to a dimmed illumination) and covering the grid floor with a plain black base plate, mice were returned into this modified, novel context. During the first 210 s, animals were allowed to freely explore, and then the auditory cue of day 1 was presented for the next 180 s (cue phase). Freezing was defined as no movement (no new beam break) for

more than 3 s and was recorded automatically in all test phases. For analysis, the percentage duration of freezing per phase was calculated. Contextual memory was obtained by subtracting the percentage of freezing during habituation from that in the context phase; memory of cue was obtained by subtracting the percentage of freezing in the novel context from that in the cue phase.

Pole Test and Rotarod/Accelerod—The pole was used as a simple test for motor-coordinative deficits. The test item consisted of a metal pole (diameter, 1.5 cm; length, 50 cm), which was wrapped with an antislip tape. The pole with a plastic ball on the top was vertically installed on a heavy platform. For testing, animals were placed head-up directly under the ball, and time to orient themselves down and descend the length of the pole was measured (cut-off time, 120 s). Aberrant activities (*e.g.* falling, jumping, and sliding) were recorded as 120 s value. The best performance over five trials was used for analysis.

The rotarod is a standard test widely used to investigate neuromotor performance in rodents. It provides a quantitative assessment of coordination and balance because animals must continuously walk on a horizontal, rotating cylinder to avoid falling off the rod. Testing was performed on two consecutive days, using a computer-controlled rotarod system (TSE Systems). In the first morning session, mice were trained on a constantly rotating rod (10 rpm) until they were able to stay on the drum for at least 60 s. In the afternoon and on the following day, three test sessions were conducted, each consisting of three trials. The rod speed was accelerated from 4 to 40 rpm over a 5-min period. The total distance moved until the animal fell down was calculated automatically by the system. Performance was examined for each testing trial (motor learning) and using best trial analysis (motor coordination).

Automated Phenotyping

Circadian pattern of locomotor activity and ingestion behavior was assessed using the PhenoMaster system (TSE Systems). Two horizontally staked infrared sensor frames detected locomotion in the *x-y* level and rearing events in the *z* level. Measurement of water and food consumption was employed by two balances. Continuous recording of these four parameters was carried out simultaneously for all mice in individual observation units (standard type III cages with grid lid) for 6 days. Data were collected automatically with a rate of 100 Hz and stored on a personal computer as a sum over 1-min intervals. The experiment took place under a 12-h light/dark cycle (lights on at 0600 h, lights off at 1800 h). Animals received water and food *ad libitum* and remained undisturbed by the investigator during observation.

Quantitative PCR Analyses

RNA was extracted from various tissues by dispersing 50–100 mg of tissue in 1 ml of TRIzol reagent (Invitrogen). Upon incubation at room temperature for 5 min, chloroform (0.2 ml) was added, and the solution was mixed for 15 s and centrifuged for 10 min at $10,000 \times g$ and 4 °C. The upper aqueous phase was transferred to a new tube, mixed with 1 volume of 70% ethanol, and applied to an RNeasy minicolumn (Qiagen, Hilden, Germany), and the RNA was purified and eluted

according to the manufacturer's instructions. 1 μg of RNA was reverse transcribed in a 20-μl reaction volume using random oligomers and SuperscriptII (Invitrogen) according to the manufacturer's directions. The reaction volume was brought to 80 μl with H_2O, and 1 μl of the cDNA solution was used for real-time PCR, which was done in duplicate in a 20-μl reaction volume using QuantiTect SYBR Green PCR Master Mix (Qiagen, Hilden). The housekeeping gene *ACTB* was used as a reference gene, and real-time PCR was performed with the murine QuantiTect primer assay *QPCTL* and murine QuantiTect primer assay *ACTB* (both from Qiagen, Hilden) on a LightCycler 2.0 system (Roche Applied Science) using preset standard protocols. The mRNA levels were analyzed by the $\Delta\Delta Ct$ method.

Primary Cell Culture

Cultures of primary neurons were prepared from mouse embryos (embryonic day 16). The brains were removed and separated in tubes with DMEM/F-12 (Invitrogen), 5% FBS (Invitrogen), 0.05% gentamycin (PAA, Pasching, Austria). Afterward, each brain was triturated with a 10-ml pipette. The cells were separated using 100- and 40-μm cell strainers (BD Biosciences) consecutively. Cells of 20 μl of solution were stained with trypan blue (Sigma), and the vital cells were counted using a Fuchs-Rosenthal counting chamber (Roth, Karlsruhe, Germany). 6×10^5 cells were spread on poly-L-lysine-coated 12-well plates and cultured at 37 °C in a humidified atmosphere containing 5% CO_2. The next day, the medium was exchanged, and cells were cultured in DMEM/F-12, 5% FBS, 0.05% gentamycin containing 25% conditioned medium from astrocyte cultures, N-2 (Invitrogen). Cytosine arabinoside (Sigma) was added (1 μM) 3 days after preparation. The cells were subjected to the respective analyses on the next day.

Astrocyte cultures were prepared from brains of newborn mice. The brains were removed, separated in tubes with DMEM/F-12 (Invitrogen), 5% FBS (Invitrogen) containing 0.05% gentamycin (PAA) and triturated using a 10-ml pipette. The brain solutions passed 100- and 40-μm cell strainers (BD Biosciences). Cells were stained with trypan blue (Sigma) and counted using a Fuchs-Rosenthal counting chamber (Roth), and 6×10^5 cells were seeded on poly-L-lysine 12-well plates. The cells were cultured at 37 °C in a humidified atmosphere containing 5% CO_2. Seven days later, the medium was renewed. The astrocytes were subjected to the analyses 12 days after seeding.

Determination of QC Activity

QC activity was determined using a discontinuous assay based on separation and quantification of the substrate Gln-βNA and the product pGlu-βNA using HPLC-UV. Briefly, test samples from brain or peripheral tissue were homogenized in a buffer consisting of 10 mM Tris, 100 mM NaCl, 5 mM EDTA, 0.5% Triton X-100, and 10% glycerol, pH 7.5, using a Precellys homogenizer (Peqlab). The homogenate was further sonicated and centrifuged at $16,000 \times g$ for 30 min and 4 °C. The protein concentration of the resulting supernatant containing QC and isoQC was adjusted to 5–7 mg/ml. Reaction samples consisted of 50 μM Gln-βNA in 25 mM MOPS, pH 7.0, 0.1 mM *N*-ethylmaleinimide, and enzyme solution in a final volume of 1 ml. The

reaction temperature was 37 °C. Test samples were removed for up to 1 h, and the reaction was stopped by boiling for 5 min followed by centrifugation at $16,000 \times g$ for 10 min. The supernatant was applied to HPLC analyses using a RP18 LiChroCART HPLC Cartridge and the HPLC system D-7000 (Merck-Hitachi). The samples (20 μl) were injected and separated by increasing the concentration of solvent A (acetonitrile containing 0.1% TFA) from 8 to 20% in solvent B (H_2O containing 0.1% TFA). QC activity was quantified from a standard curve of pGlu-βNA (Bachem) determined under assay conditions.

Immunohistochemistry

Mice ($QC^{-/-}$ and wild type littermates) were euthanized with carbon dioxide and perfused transcardially with phosphate-buffered saline (PBS). The brains were dissected, cut into sample pieces ($\sim 3 \times 5$ mm), and immersion-fixed with HOPE® (hepes glutamic acid buffer-mediated organic solvent protection effect, DCS Diagnostics, Hamburg, Germany), following the manufacturer's instructions. Coronal sections of 10 μm were cut from the paraffin blocks using a sliding microtome and transferred to microscope slides. For antigen retrieval, the slides were incubated in hot citrate buffer (~ 95 °C/30 min). Endogenous peroxidase was inactivated with 0.5% H_2O_2 in TBS containing 0.25% Triton X-100 (10 min). Nonspecific binding sites were blocked with 5% normal goat serum in TBS containing 0.25% Triton X-100 (1 h). As primary antibody, a polyclonal rabbit antibody (mQC1302, 1:200) was used at 4 °C overnight in antibody dilution buffer (DCS Diagnostics). As secondary antibody, biotinylated goat anti-rabbit antibody (1:1,000; Vector Laboratories) was used (1 h at room temperature). A Vectastain kit (Vector Laboratories) was used for the ABC method. The immunoreaction was visualized with DAB-Ni (DAB substrate kit for peroxidase; Vector Laboratories) (3 min).

Determination of Testosterone, Thyroxine, TSH, and GnRH by ELISA

The serum T4 and testosterone concentrations were analyzed to evaluate potential effects of the QC knock-out on the HPT or HPG axis. Competitive ELISAs were used according to the recommendations of the manufacturer (IBL International, Hamburg, Germany). The concentration of GnRH in serum and hypothalamic homogenates was determined applying an ELISA from Peninsula Laboratories (San Carlos, CA). Serum TSH was quantified using an ELISA from Gentaur (Brussels, Belgium).

Oral Glucose Tolerance Test

Before oral glucose load, mice were fasted for 5 h. Glucose (3 g/kg of a 40% glucose solution) was administered by oral gavage (with a feeding needle, 22 gauge, 25 mm; Fine Science Tools, Heidelberg, Germany) at 0 min. The blood glucose and insulin concentration was assessed for 120 min. Insulin concentrations were determined using commercial ELISAs (Mercodia AB; Uppsala, Sweden).

RESULTS

Generation and Characterization of QC Knock-out Animals—The generation of a constitutive QC knock-out model has been achieved by flanking the targeted region with two LoxP sites, allowing its ubiquitous or tissue-specific deletion, depending on Cre-recombinase action. Based on the functional data obtained in former studies, it was decided to target exons 4 and 5 of the QC gene, which contain several essential residues of the active site. Following preparation of the targeting vector and selection of targeted ES cells, ES cells were inserted into blastocysts, and chimeric mice were obtained. After mating of the chimeras with Cre-expressing transgenic mice, heterozygous QC knock-out mice were selected. Inter-cross-breeding and genotyping of the offspring allowed the identification of constitutive homozygous knock-out ($QC^{-/-}$) animals (Fig. 1A).

QC protein expression in knock-out mice was assessed by determination of activity and immunohistochemistry. An analysis of QC activity in different tissues of the mice revealed a high expression in the brain, liver, and spleen, lower expression in muscle, and no detectable activity in peripheral organs like the kidney and heart (Fig. 1B). A comparison with the activity observed in $QC^{-/-}$ animals revealed a significant decrease of QC activity in the brain, but not in the liver and spleen. Because the determination of the activity does not discriminate between the enzyme and isoenzyme, it appears very likely that isoQC is the primary enzyme in peripheral tissues. The remarkable expression of QC in the brain was further analyzed by QC immunohistochemistry (Fig. 1C) and determination of activity in several regions of the cerebrum and the cerebellum (Fig. 1D). Both analyses provided similar results. In immunohistochemistry, wild type animals showed an immunostaining in cortical and hippocampal brain regions, which was prominent in the regions CA1 to -3 and the dentate gyrus of the hippocampus. The staining was clearly diminished in $QC^{-/-}$ animals. Accordingly, the highest QC activity was observed in hypothalamus and hippocampus of wild type mice, which was significantly diminished in $QC^{-/-}$, suggesting QC as the primary source of the activity in these brain regions. Lower QC activity was observed in cerebellum and cortex. Interestingly, the residual enzymatic activity in the knock-out animals appeared to be similar, which suggests a basal expression of the isoenzyme and a more differential expression of QC (15). In order to further investigate the cellular origin of QC activity in the brain, primary cortical neurons were cultured. Neurons from wild type mice secreted QC activity into the culture medium, which is in agreement with earlier investigations using transfected cultured cells. QC secretion decreased gene dose-dependently in primary neurons from $QC^{-/-}$ animals, supporting that the secreted activity is only caused by QC and not by isoQC (Fig. 1E). Similarly, QC activity was also detected in the medium of cultured glia cells, and the activity was abolished in glia medium from $QC^{-/-}$ mice. In contrast to the activity in the media, the QC activity did not change in the cell pellet, which suggests that the Golgi-resident isoQC activity is present and accounts for the majority of the activity within the cells. The gene dose-dependent reduction of QC in the medium of the cultured primary cells corresponds to the abolishment of QC activity in plasma of $QC^{-/-}$ (Fig. 1F). Thus, depletion of a functional QC gene results primarily in an effect on the extracellular QC activity.
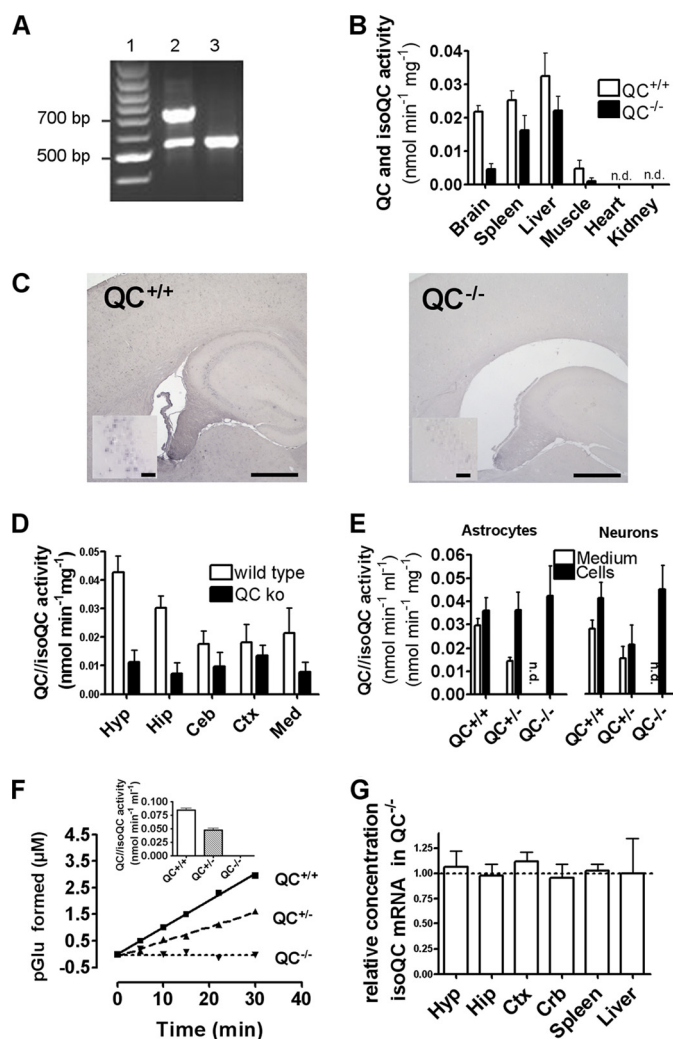
FIGURE 1. **Characterization of QC expression and activity in mouse line pbd-02 (QC knock-out).** *A*, representative PCR analysis for offspring genotyping of line pbd-02. The 525 bp band corresponds to the knock-out allele, and the 725 bp band corresponds to the wild type allele. Genotyping results for a heterozygous animal (*lane 2*) and a homozygous knock-out animal (*lane 3*) are shown. *B*, characterization of the specific QC activity in brain and peripheral tissues of $QC^{+/+}$ and $QC^{-/-}$ mice ($n = 4$–7 mice/genotype; *n.d.*, not reliably detectable). Mice had an age of 3–4 months at sacrifice. The most pronounced reduction of QC activity was observed in the brain. *C*, immunohistochemical analysis of the hippocampal region, applying a polyclonal antiserum against QC (*scale bars*, 500 mm; *inset* of the CA3 region, 50 mm). *D*, characterization of the specific QC activity in different brain regions, depending on the genotype ($n = 5$–7 mice/genotype). *Hyp*, hypothalamus; *Hip*, hippocampus; *Ceb*, cerebellum; *Ctx*, cortex; *Med*, medulla. *E*, QC activity in primary neuronal cells from $QC^{+/+}$, $QC^{+/-}$, and $QC^{-/-}$ cells. Neurons and glial cells secrete QC into the medium. Conditioned medium of $QC^{-/-}$ cells is devoid of QC activity. The intracellular QC activity does not change significantly, suggesting that the activity of the Golgi-localized isoQC is not up-regulated ($n = 3$–4 mice/genotype). *F*, QC-activity in the plasma of mouse line pbd-02. The activity drops gene dose-dependently, similar to what was observed in the primary cell culture. Plasma of $QC^{-/-}$ mice is devoid of QC activity ($n = 4$–8 mice/genotype). *G*, quantitative PCR analysis of isoQC transcripts in different tissues, depending on the genotype. The transcript levels of isoQC do not differ in the tissues, suggesting the absence of a compensatory up-regulation of isoQC due to QC depletion ($n = 4$ mice/genotype). All *bar graphs* are shown as mean ± S.E. (*error bars*).

Finally, we investigated the expression of isoQC using real-time PCR, in order to exclude a compensatory up-regulation of isoQC. A direct comparison of the RT-PCR results obtained for isoQC did not reveal an increase of the transcript levels of isoQC in $QC^{-/-}$ animals (Fig. 1*G*). Thus, the determination of

the QC activity is most likely not hampered by an increase in isoQC activity, which potentially shadows the decrease in activity in the $QC^{-/-}$ mice. Finally, this is also supported by the similar intracellular QC concentration/activity in the primary neuronal cells (Fig. 1*E*), which is most likely caused by isoQC.

Phenotypic Analysis—The QC knock-out animal colony was expanded by intercross of $QC^{+/-}$ mice. Among 955 pups, 24% were homozygous for the QC knock-out allele, which is in accordance with an expected Mendelian heredity and indicates the absence of prenatal lethality.

In order to assess potential phenotypic differences between QC knock-out mice and wild type littermates, a group of young adult males was subjected to a comprehensive phenotypic assessment. A comparison of the body weight of the animals in the three genotype groups revealed a tendency to a reduced weight of $QC^{-/-}$ mice (Fig. 2*A*). However, the differences were not statistically significant, and the effect was not gene dose-dependent. Weight gain was virtually identical among all genotypes.

The behavioral assessment of the mice was initiated by a primary screen investigating the animals' general behavior and health status in a qualitative assessment. No abnormalities were detected in $QC^{+/-}$ or $QC^{-/-}$ mice (not shown). Animals were further characterized in an automated phenotyping assessment in order to observe potential behavioral changes in a consecutive manner for 136 h. The phenotyping system allowed quantification of locomotion as well as food and water consumption (Fig. 2, *B* and *D*) and examination of the day/night rhythm of activity (Fig. 2*C*) and feeding. Supporting the primary screen result, no difference in food or water consumption was observed between all groups. Furthermore, the general locomotor activity was identical in all groups, and also the rhythm of day and night activity did not reveal differences between genotypes. Likewise, an assessment of the mice in a rotarod paradigm as well as in the pole assay did not reveal a difference in the motor function of the $QC^{-/-}$ mice (Fig. 2, *E* and *F*).

Finally, the cognitive function of the animals was investigated in a fear conditioning paradigm. $QC^{-/-}$ mice displayed a virtually identical freezing behavior in contextual and cued memory assessment compared with wild type littermates (Fig. 2, *G* and *H*), suggesting no influence of the QC depletion on the hippocampus/amygdala-dependent associative memory.

Characterization of HPG Axis and Stability of GnRH—The hypothalamic pGlu hormone GnRH stimulates secretion of pituitary hormones into the blood, which finally results in peripheral production of steroid hormones (*e.g.* testosterone). The activity of GnRH has been shown to depend on the N terminus (20). Hypogonadal (*hpg*) mice, which have been shown to lack GnRH, are not fertile and do not show testosterone production (21). A significantly affected HPG axis was not expected in $QC^{-/-}$ mice due to proven fertility. Indeed, the GnRH concentration in serum of $QC^{-/-}$ mice did not differ from that of $QC^{+/+}$ mice, suggesting that processing of the potential QC substrate remained unaltered (Fig. 3*A*). Accordingly, also the concentration of testosterone in serum of $QC^{+/+}$ and $QC^{-/-}$ did not show a significant difference (Fig. 3*B*). Similarly, the mRNA concentration of GnRH in the hypothalamus and of LH and FSH in the pituitary was virtually identical
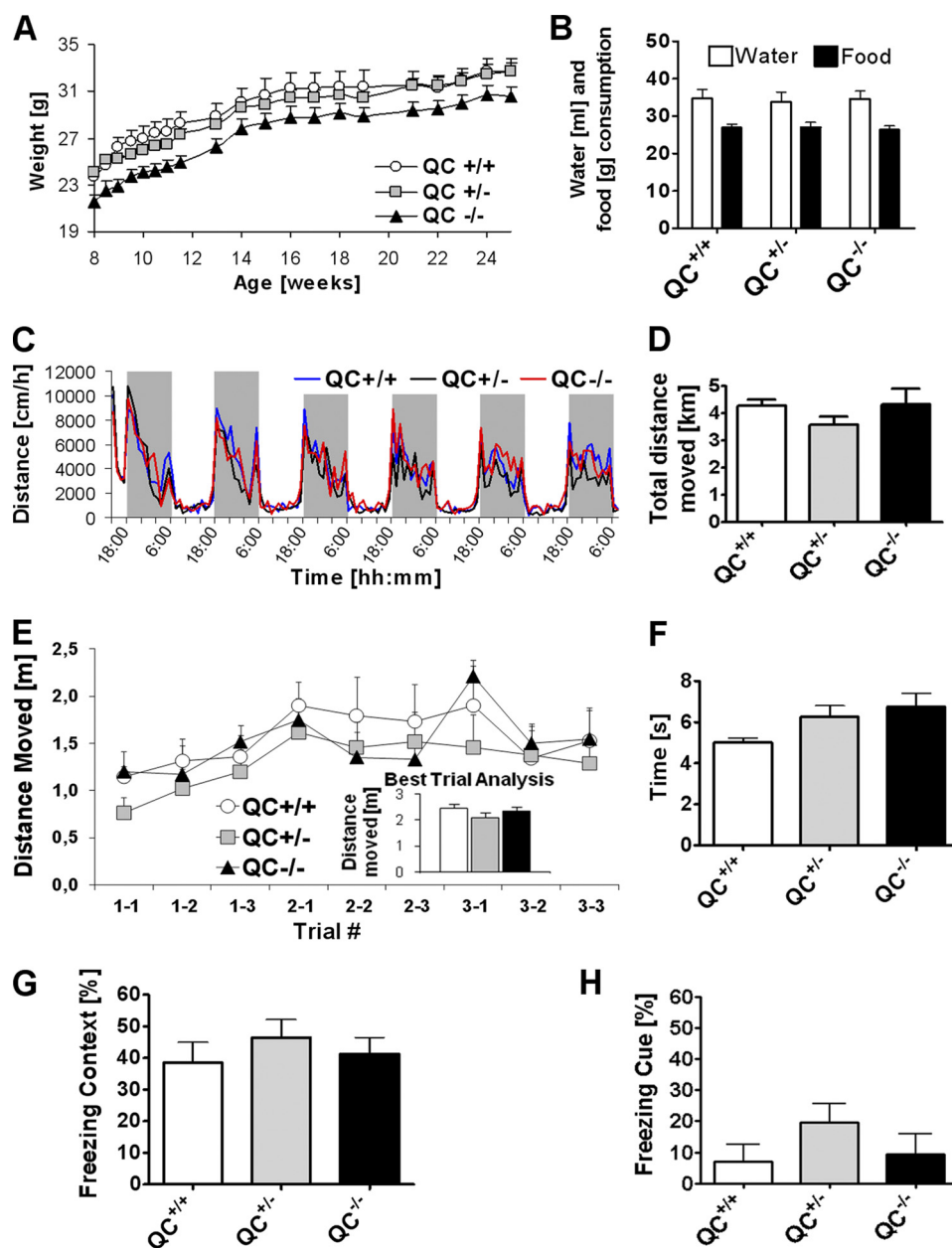
FIGURE 2. **Phenotypic assessment of male mice of mouse line pbd-02.** *A*, weight gain of QC$^{+/+}$, QC$^{+/-}$, and QC$^{-/-}$ mice. QC$^{-/-}$ mice display a tendency to be smaller, but gain in weight is virtually identical to that in wild type and heterozygous QC knock-out mice ($n = 7-12$, mean $\pm$ S.E. (*error bars*)). *B–D*, behavioral phenotyping data from a fully automated home cage assessment of young adult mice (age 4 months, $n = 8$ mice/group; *bar graphs*, mean $\pm$ S.E. for 136 h. The consumption of food and water (*B*), locomotor activity patterns during 12-h light/12-h dark cycles (*C*), and also the total distance moved within the period of investigation (*D*) was virtually identical among all groups. *E*, assessment of motor function and learning in a rotarod trial. No differences are observed in the consecutive trial analysis and the best trial analysis (*inset*) (4 months, $n = 8-12$ mice/genotype, mean $\pm$ S.E.). *F*, evaluation of general motor function in a pole test paradigm. In accordance to the findings in the rotarod and automated phenotyping, no differences were observed between the groups ($n = 8-12$, mean $\pm$ S.E.). *G* and *H*, analysis of cognitive performance of QC$^{+/+}$, QC$^{+/-}$, and QC$^{-/-}$ mice in a fear conditioning paradigm. Freezing times were analyzed in response to re-exposure to the context of conditioning (*G*) and following the cue (*H*) (tone), reflecting associative learning. Differences between genotype groups did not reach statistical significance ($n = 8-12$, age 4.5 months, mean $\pm$ S.E.).

(supplemental Figs. S1 and S2). In order to gain further insight into the role of the N-terminal pGlu for stability of the hormone in serum, we synthesized GnRH containing an N-terminal glutaminyl or pGlu residue. The incubation of the native, pGlu-modified peptide did not result in any signs of degradation up to 2 h (Fig. 3*C*). In strong contrast, a rapid N-terminal degradation was observed if Gln^1-GnRH was incubated in serum of QC$^{-/-}$ mice (Fig. 3*D*). The observed peptide fragments suggest a stepwise N-terminal cleavage following the initial removal of the

glutaminyl residue. If Gln^1-GnRH was incubated in serum of wild type mice, two processes were observed: partial degradation by aminopeptidases and N-terminal pGlu formation by QC present in serum (not shown). The data imply that a secretion of significant amounts of immature GnRH does not occur in QC$^{-/-}$ mice, probably because of compensatory pGlu formation.

Characterization of HPT Axis—TRH (pGlu-His-Pro-amide) is produced by hypothalamic neurons, stimulating TSH pro-
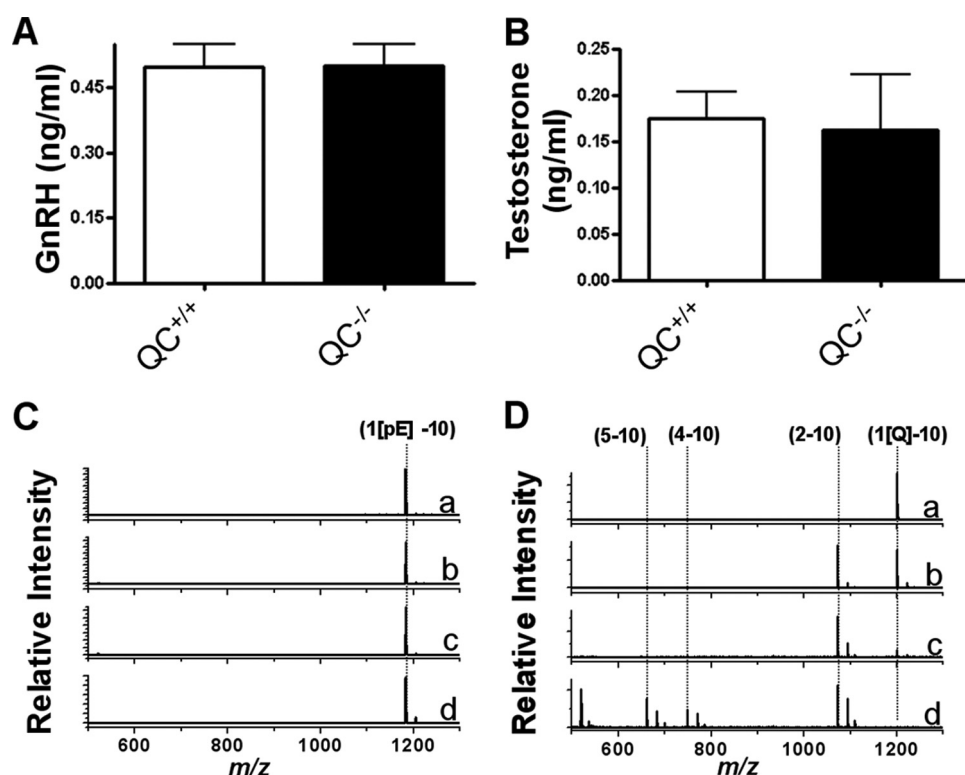
FIGURE 3. **Influence of the genotype of mouse line pbd-02 on hormones of the HPG axis.** *A*, GnRH concentration in serum of male pbd-02 mice ($QC^{+/+}$, *n* = 33; $QC^{-/-}$, *n* = 30). *B*, testosterone concentration in serum of male pbd-02 mice ($QC^{+/+}$, *n* = 34; $QC^{-/-}$, *n* = 30). *C* and *D*, degradation of GnRH in 25% serum of $QC^{-/-}$ mice, assessed using MALDI-TOF mass spectrometry. pGlu-GnRH (*1[pE]-10* in *C*) remained stable over a 2-h time period. In contrast, Gln^1-GnRH (*1[Q]-10*) displayed a significant instability under identical conditions (*C* and *D*; time points are 0 (*a*), 2 (*b*), 30 (*c*), and 120 min (*d*)).

duction in the pituitary and, by that, stimulating secretion of the thyroid hormones. The physiological function of TRH depends strongly on the N-terminal pGlu residue (22). Due to the noteworthy instability of pGlu-TRH in the circulation (half-life below 10 min) (23), a direct determination in plasma is not feasible. However, the HPT axis hormones TSH and T4 are the major mediators of TRH in the periphery, and therefore the concentration of the other axis hormones is used to mirror the effect of TRH *in vivo* (24, 25). The depletion of QC resulted in a statistically significant decrease of the serum T4 concentration in male $QC^{+/-}$ and $QC^{-/-}$ mice by 20 and 24%, respectively (Fig. 4*A*; $p < 0.01$). The concentration of TSH in serum was decreased in male $QC^{+/-}$ mice but similar in $QC^{+/+}$ and $QC^{-/-}$ mice (Fig. 4*B*). The TSH changes lacked statistical significance. In female mice, increased concentrations of TSH were observed in $QC^{-/-}$, and the drop of T4 was smaller compared with male mice (supplemental Fig. S3). A histological analysis of the thyroid gland did not reveal significant abnormalities. A tendency to a smaller and rod-shaped nuclei in $QC^{-/-}$ compared with $QC^{+/+}$ mice (Fig. 4*C*) might indicate a lower transcriptional activity, which would corroborate the results of the T4 ELISA analysis.

For a comparison with our QC knock-out line pbd-02, TRH knock-out mice (25) showed a doubling of serum TSH, accompanied by a 50% reduction of the serum T4 and significantly impaired glucose tolerance. Notably, tests of oral glucose tolerance and insulin secretion of $QC^{-/-}$ mice did not reveal any impairment, supporting a very restricted effect on the HPT axis (Fig. 4, *D* and *E*).

Blood Cell Analysis—In a final assessment, we analyzed several blood parameters in male and female $QC^{+/+}$ and $QC^{-/-}$ mice (Table 1). None of the parameters showed a significant difference between genotypes analyzed.

DISCUSSION

Although the N-terminal pGlu modification of peptides has been known for more than a century, the role of the residue in many proteins and its generation by QCs are still not well understood. More recent studies also suggest an important function of pGlu-modified amyloid peptides in neurodegenerative disorders like Alzheimer disease and familial Danish dementia or familial British dementia (11, 26–28). The inhibition of QC by applying orally available inhibitors attenuated the Alzheimer disease-like pathology in transgenic mouse models (11). For development of therapeutics, however, an influence on conversion of QC substrates (*e.g.* neuropeptides) has to be considered. Therefore, QC knock-out animals were generated and characterized to gain further insights into the enzyme expression and conversion of physiological substrates and to reveal potential target-specific side effects.

Interestingly, the majority of QC activity in brain tissue is caused by QC, and only a minor proportion is caused by isoQC. The abundance of QC in hypothalamus (*i.e.* a brain region with high expression of its potential substrates TRH and GnRH) links QC expression with sites of high pGlu peptide generation and secretion (18). Moreover, the expression of QC in medulla and hippocampus as shown here matches well with the sites of synthesis of the pGlu peptides neurotensin and orexin. Thus, it
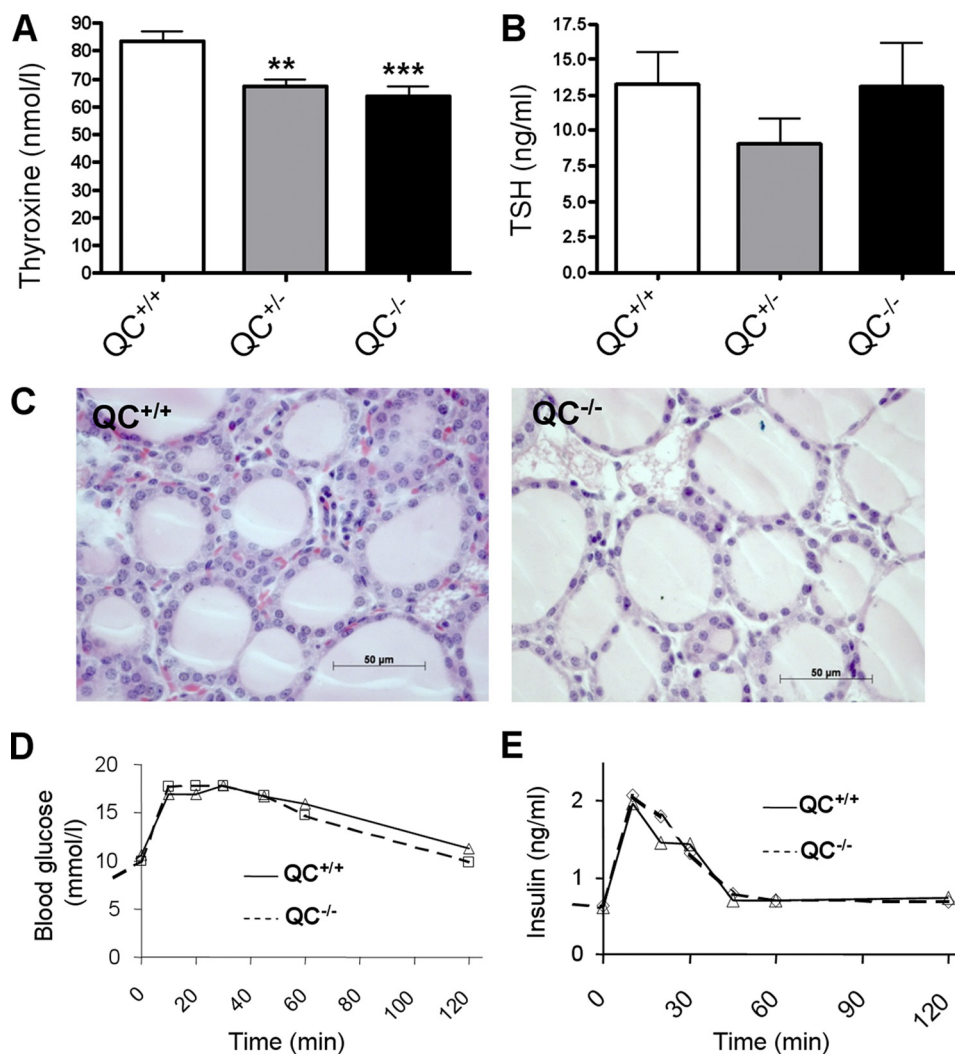
FIGURE 4. **Influence of the genotype of mouse line pbd-02 on hormones of the HPT axis.** *A*, T4 concentration in serum of male pbd-02 mice (QC$^{+/+}$, $n = 20$; QC$^{+/-}$, $n = 20$; QC$^{-/-}$, $n = 15$; **, $p < 0.01$; ***, $p < 0.001$). *B*, TSH concentration in serum of male pbd-02 mice (QC$^{+/+}$, $n = 17$; QC$^{+/-}$, $n = 20$; QC$^{-/-}$, $n = 14$). The lowering did not reach statistical significance. *C*, histopathological analysis of QC$^{+/+}$ and QC$^{-/-}$. The *smaller size* and *oval shape* of the nuclei in QC$^{-/-}$ indicates lower transcriptional activity. *D*, oral glucose tolerance test of QC$^{+/+}$ and QC$^{-/-}$. The differences lacked statistical significance, also with regard to area under the curve (not shown). *E*, insulin concentration in plasma (QC$^{+/+}$, $n = 15$; QC$^{-/-}$, $n = 15$).

TABLE 1
Blood parameters in male and female QC$^{+/+}$ and QC$^{-/-}$ mice

	White blood cells	Red blood cells	Platelets	Hemoglobin	Hematocrit	mcv[a]
	$\times 10^3/mm^3$	$\times 10^6/mm^3$	$\times 10^3/mm^3$	*g/dl*	*%*	*fl/cell*
Male WT	10.63 ± 1.27	9.02 ± 1.93	416.4 ± 219.59	13.98 ± 2.72	44.16 ± 8.28	49.4 ± 1.86
Male homozygous	11.74 ± 2.49	9.78 ± 0.46	358.2 ± 92.6	15.04 ± 0.67	47.45 ± 2.23	48.6 ± 0.49
Female WT	8.96 ± 2.6	10.2 ± 0.36	227.4 ± 67.1	15.57 ± 0.66	49.16 ± 2.46	48.2 ± 1.17
Female homozygous	10.4 ± 2.47	8.82 ± 1.18	265.4 ± 81.4	15.54 ± 1.4	47.15 ± 1.48	55.6 ± 11.18
	mchc[b]	mpv[c]	Lymphocytes	Monocytes	Granulocytes	Eosinophils
	g/dl	*fl/cell*	$\times 10^3/mm^3$	$\times 10^3/mm^3$	$\times 10^3/mm^3$	$\times 10^3/mm^3$
Male WT	31.61 ± 0.49	6.45 ± 0.6	4.3 ± 2.27	1 ± 0.52	2.98 ± 1.82	0.32 ± 0.26
Male homozygous	31.71 ± 0.1	6.29 ± 0.36	5.76 ± 1.22	1.4 ± 0.26	4.56 ± 1.1	0.68 ± 0.31
Female WT	31.67 ± 0.42	6.44 ± 0.4	3.54 ± 2.18	0.78 ± 0.48	2.3 ± 1.39	0.34 ± 0.22
Female homozygous	32.89 ± 1.98	6.78 ± 0.36	4.26 ± 2.61	1.04 ± 0.55	2.75 ± 1.51	0.44 ± 0.34

[a] Mean corpuscular volume.
[b] Mean corpuscular hemoglobin concentration.
[c] Mean platelet volume.

appears that the differential expression of QC in the brain might be related to production of its substrates (*i.e.* neuropeptides). These hormones are expressed via the regulated secretory pathway and secreted upon extracellular stimuli. The maturation of the peptide precursors has been described as taking place in the secretory compartments, containing prohormone convertases and peptidylglycine-α amidating monooxygenase (29–32). The secretion of QC from primary cells (Fig. 1) sup-

ports its presence in the secretory pathway of neurons, which was also suggested recently by immunofluorescent double labelings of QC with compartment-specific marker proteins in mouse brain (33). The link between QC activity, neuropeptide maturation, and secretion is finally supported by the presence of GnRH and QC in serum, as shown here for the first time. The co-localization within secretory granules and co-secretion appears conceivable because the maturation of the N terminus by QC is only accomplished after cleavage by convertases. Formation of pGlu represents therefore a finishing step in the process of N-terminal peptide maturation.

In contrast to QC, isoQC remains intracellulary localized, as shown here in primary cells (Fig. 1). Both enzymes share virtually identical catalytic characteristics, and isoQC might, therefore, still contribute to pGlu-formation before secretion of the substrates. Other studies gave rise to the assumption that most of the substrates of QC and isoQC appear to be secreted in their mature form (*i.e.* containing the pGlu residue at the N terminus) (29, 34, 35). An extracellular activity of QC might be, therefore, not important for the general maturation process. Thus, isoQC, which is apparently not secreted from the expressing cells in an active form (15) (Fig. 1*E*), might indeed complement the absence of QC to a certain extent. The N- and C-terminal maturation of peptide hormone precursors is initiated in the Golgi compartment of the cells. This, in turn, could involve partially isoQC-mediated pGlu formation at the N terminus of neuropeptides. Moreover, our *in vitro* investigations of a spontaneous cyclization of glutamine point to a half-life of N-terminal glutamine of about 3–6 days (13). Thus, in addition, a small portion of the peptides generated in the secretory granules might be converted into pGlu peptides by a spontaneous process, a reaction, which was thought to be the general cause of pGlu formation prior to the discovery of the QCs (36).

Both processes, a partial complementation by the isoQC and a spontaneous formation of pGlu from the precursors, might lead to a generation of a sufficiently high concentration of the pGlu neuropeptides without affecting the general physiology, as suggested by the behavioral analysis (Figs. 2 and 3 and Table 1). In this regard, the phenotypic and clinical assessments were arranged to monitor potential hormonal or proteinogenic dysfunctions of pGlu protein-regulated processes. For instance, the hippocampal hormone orexin A mediates the rhythm of day/night activity. Intracerebral injection of orexin A has been shown to increase activity and amyloid β production (37). Because we did not observe a difference in automated phenotyping, the orexin activity does not appear to be significantly influenced. Furthermore, many proteins bearing a pGlu residue are components of the extracellular matrix (*e.g.* collagens or fibronectin) (38). Influencing their function would be expected to result in abnormalities in motor function. Finally, neuropeptides like neurotensin have been described as influencing cognition (39). At least in one paradigm to assess spatial and pain-associated memory, QC-deficient mice were indistinguishable from wild type littermates.

Support for a significant pGlu neuropeptide formation in the absence of QC is also provided by the analyses of the hormones of the HPG and HPT axis, which are modulated by the hypothalamic hormones GnRH and TRH, respectively. Previous studies clearly showed that the activity and stability of these peptides depends on the N-terminal pGlu residue (20, 22, 23, 40, 41). Our analyses point to a mild hypothyroidism caused by QC depletion, as mainly suggested by the lowering of the T4 concentration. In contrast, we could not obtain any sign of a hypogonadism, which would be caused by reduced GnRH concentrations. In addition, the pGlu residue is an important mediator of peptide stability, as shown here by the *ex vivo* degradation in serum (23).

The differential effect on the hypothalamic hormones TRH and GnRH might be caused by differing potency of isoQC to complement the pGlu formation (scheme in supplemental Fig. S4). In contrast to TRH, the N-terminal maturation of GnRH apparently does not depend on prohormone convertase cleavage (*i.e.* signal peptidase generates the N-terminal glutaminyl residue prone to cyclization). Because the cyclization can occur in the ER and Golgi compartment, isoQC is capable of conducting pGlu formation and compensating for loss of QC efficiently. In contrast, it is expected that the majority of TRH is generated by prohormone convertases in secretory granules (29). Therefore, N-terminal maturation is more sensitive to loss of QC activity (supplemental Fig. S4).

The absence of serious phenotypic and physiological changes of QC$^{-/-}$ mice (at the time of preparation of this report, the oldest animals had an age of 12 months and did not show any sign of illness) raises novel implications for drug development. The present study shows that a depletion of the *QPCT* gene does not result in abnormalities in behavior and results in only restricted changes in hormonal homeostasis. The results support the therapeutic approach of QC inhibition in chronic neurodegenerative diseases, such as Alzheimer disease, familial British dementia, and familial Danish dementia. Although several pGlu neuropeptides regulate the general physiological function, a broad therapeutic window for reduction of the total QC activity appears without affecting the physiology. Future studies will concentrate on the differential roles of QC and isoQC by generation of isoQC knock-out mice in order to dissect a potential differential function of the proteins.

REFERENCES

1. Awadé, A. C., Cleuziat, P., Gonzalès, T., and Robert-Baudouy, J. (1994) *Proteins* **20,** 34–51
2. Garavelli, J. S. (2000) *Nucleic Acids Res.* **28,** 209–211
3. Abraham, G. N., and Podell, D. N. (1981) *Mol. Cell Biochem.* **38,** 181–190
4. Van Coillie, E., Proost, P., Van Aelst, I., Struyf, S., Polfliet, M., De Meester, I., Harvey, D. J., Van Damme, J., and Opdenakker, G. (1998) *Biochemistry* **37,** 12672–12680
5. Gong, J. H., and Clark-Lewis, I. (1995) *J. Exp. Med.* **181,** 631–640
6. Schlenzig, D., Manhart, S., Cinar, Y., Kleinschmidt, M., Hause, G., Willbold, D., Funke, S. A., Schilling, S., and Demuth, H. U. (2009) *Biochemistry* **48,** 7072–7078
7. Schilling, S., Lauber, T., Schaupp, M., Manhart, S., Scheel, E., Böhm, G., and Demuth, H. U. (2006) *Biochemistry* **45,** 12393–12399

8. Tomidokoro, Y., Lashley, T., Rostagno, A., Neubert, T. A., Bojsen-Møller, M., Braendgaard, H., Plant, G., Holton, J., Frangione, B., Révész, T., and Ghiso, J. (2005) *J. Biol. Chem.* **280,** 36883–36894

9. D'Arrigo, C., Tabaton, M., and Perico, A. (2009) *Biopolymers* **91,** 861–873

10. He, W., and Barrow, C. J. (1999) *Biochemistry* **38,** 10871–10877

11. Schilling, S., Zeitschel, U., Hoffmann, T., Heiser, U., Francke, M., Kehlen, A., Holzer, M., Hutter-Paier, B., Prokesch, M., Windisch, M., Jagla, W., Schlenzig, D., Lindner, C., Rudolph, T., Reuter, G., Cynis, H., Montag, D., Demuth, H. U., and Rossner, S. (2008) *Nat. Med.* **14,** 1106–1111

12. Schilling, S., Appl, T., Hoffmann, T., Cynis, H., Schulz, K., Jagla, W., Friedrich, D., Wermann, M., Buchholz, M., Heiser, U., von Hörsten, S., and Demuth, H. U. (2008) *J. Neurochem.* **106,** 1225–1236

13. Seifert, F., Schulz, K., Koch, B., Manhart, S., Demuth, H. U., and Schilling, S. (2009) *Biochemistry* **48,** 11831–11833

14. Pohl, T., Zimmer, M., Mugele, K., and Spiess, J. (1991) *Proc. Natl. Acad. Sci. U.S.A.* **88,** 10059–10063

15. Cynis, H., Rahfeld, J. U., Stephan, A., Kehlen, A., Koch, B., Wermann, M., Demuth, H. U., and Schilling, S. (2008) *J. Mol. Biol.* **379,** 966–980

16. Busby, W. H., Jr., Quackenbush, G. E., Humm, J., Youngblood, W. W., and Kizer, J. S. (1987) *J. Biol. Chem.* **262,** 8532–8536

17. Fischer, W. H., and Spiess, J. (1987) *Proc. Natl. Acad. Sci. U.S.A.* **84,** 3628–3632

18. Böckers, T. M., Kreutz, M. R., and Pohl, T. (1995) *J. Neuroendocrinol.* **7,** 445–453

19. Rogers, D. C., Fisher, E. M., Brown, S. D., Peters, J., Hunter, A. J., and Martin, J. E. (1997) *Mamm. Genome* **8,** 711–713

20. Sealfon, S. C., Weinstein, H., and Millar, R. P. (1997) *Endocr. Rev.* **18,** 180–205

21. Mason, A. J., Hayflick, J. S., Zoeller, R. T., Young, W. S., 3rd, Phillips, H. S., Nikolics, K., and Seeburg, P. H. (1986) *Science* **234,** 1366–1371

22. Goren, H. J., Bauce, L. G., and Vale, W. (1977) *Mol. Pharmacol.* **13,** 606–614

23. Morty, R. E., Bulau, P., Pellé, R., Wilk, S., and Abe, K. (2006) *Biochem. J.* **394,** 635–645

24. Yamada, M., Satoh, T., and Mori, M. (2003) *Thyroid* **13,** 1111–1121

25. Yamada, M., Saga, Y., Shibusawa, N., Hirato, J., Murakami, M., Iwasaki, T., Hashimoto, K., Satoh, T., Wakabayashi, K., Taketo, M. M., and Mori, M. (1997) *Proc. Natl. Acad. Sci. U.S.A.* **94,** 10862–10867

26. Piccini, A., Russo, C., Gliozzi, A., Relini, A., Vitali, A., Borghi, R., Giliberto, L., Armirotti, A., D'Arrigo, C., Bachi, A., Cattaneo, A., Canale, C., Torrassa, S., Saido, T. C., Markesbery, W., Gambetti, P., and Tabaton, M. (2005) *J. Biol. Chem.* **280,** 34186–34192

27. Saido, T. C., Yamao-Harigaya, W., Iwatsubo, T., and Kawashima, S. (1996) *Neurosci. Lett.* **215,** 173–176

28. Saido, T. C., Iwatsubo, T., Mann, D. M., Shimada, H., Ihara, Y., and Kawashima, S. (1995) *Neuron* **14,** 457–466

29. Nillni, E. A., and Sevarino, K. A. (1999) *Endocr. Rev.* **20,** 599–648

30. Steiner, D. F. (1998) *Curr. Opin. Chem. Biol.* **2,** 31–39

31. Rehfeld, J. F. (2006) *J. Mol. Med.* **84,** 544–550

32. Wetsel, W. C., and Srinivasan, S. (2002) *Prog. Brain Res.* **141,** 221–241

33. Hartlage-Rübsamen, M., Staffa, K., Waniek, A., Wermann, M., Hoffmann, T., Cynis, H., Schilling, S., Demuth, H. U., and Rossner, S. (2009) *Int. J. Dev. Neurosci.* **27,** 825–835

34. Nillni, E. A. (1999) *Endocrine* **10,** 185–199

35. Keire, D. A., Vincent Wu, S., Diehl, D. L., Chew, P., Ho, F. J., Davis, M. T., Lee, T. D., Shively, J. E., Walsh, J. H., and Reeve, J. R., Jr. (2003) *Regul. Pept.* **113,** 115–124

36. Blomback, B. (1967) *Biochim. Biophys. Acta* **11,** 398–411

37. Kang, J. E., Lim, M. M., Bateman, R. J., Lee, J. J., Smyth, L. P., Cirrito, J. R., Fujiki, N., Nishino, S., and Holtzman, D. M. (2009) *Science* **326,** 1005–1007

38. Garcia-Pardo, A., Pearlstein, E., and Frangione, B. (1983) *J. Biol. Chem.* **258,** 12670–12674

39. Kinkead, B., Dobner, P. R., Egnatashvili, V., Murray, T., Deitemeyer, N., and Nemeroff, C. B. (2005) *J. Pharmacol. Exp. Ther.* **315,** 256–264

40. Okada, Y., Kitamura, K., Baba, Y., Arimura, A., and Schally, A. V. (1973) *Biochem. Biophys. Res. Commun.* **53,** 1180–1186

41. Karten, M. J., and Rivier, J. E. (1986) *Endocr. Rev.* **7,** 44–66